

Generalized Magneto-thermoelasticity in a Fiber-Reinforced Anisotropic Half-Space

Ibrahim A. Abbas · Abo-el-nour N. Abd-alla ·
Mohamed I. A. Othman

Received: 10 March 2010 / Accepted: 3 March 2011 / Published online: 17 March 2011
© Springer Science+Business Media, LLC 2011

Abstract The propagation of plane waves in a fiber-reinforced, anisotropic thermoelastic half-space proposed by Lord–Shulman under the effect of a magnetic field is discussed. The problem has been solved numerically using a finite element method. Numerical results for the temperature distribution, the displacement components, and the thermal stress are given and illustrated graphically. Comparisons are made with the results predicted by the theory of generalized thermoelasticity with one relaxation time for different values of time. It is found that the reinforcement has a great effect on the distribution of field quantities.

Keywords Anisotropic material · Fiber-reinforced · Finite element method · Generalized magneto-thermoelasticity

1 Introduction

Lord and Shulman [1] introduced a theory of generalized thermoelasticity with one relaxation time for an isotropic body. The theory was extended for an anisotropic

I. A. Abbas (✉) · A. N. Abd-alla
Department of Mathematics, Faculty of Science, Jazan University, Jazan, Saudi Arabia
e-mail: ibrabbas7@yahoo.com

I. A. Abbas · A. N. Abd-alla
Department of Mathematics, Faculty of Science, Sohag University, Sohag, Egypt

M. I. A. Othman
Department of Mathematics, Faculty of Science, Zagazig University, Zagazig, Egypt

M. I. A. Othman
Department of Mathematics, Faculty of Science, Shaqra University, AL-Dawadmi, Saudi Arabia
e-mail: m_i_othman@yahoo.com

body by Dhaliwal and Sherief [2]. In this theory, a modified law of heat conduction including both the heat flux and its time derivatives replaces the conventional Fourier's law. The heat equation associated with this theory is hyperbolic and hence eliminates the paradox of infinite speeds of propagation inherent in both coupled and uncoupled theories of thermoelasticity. Erdem [3] derived the heat conduction equation for a composite rigid material containing an arbitrary distribution of fibers. The impact of earthquakes on the artificial structures is of great concern to engineers and architects. During an earthquake and similar disturbances, a structure is excited into a more or less violent vibration, with resulting oscillatory stresses, which depend upon both ground vibration and physical properties of the structure. Most concrete structures need steel reinforcing to some extent. The study of plane and surface wave propagation in thermally conducting fiber-reinforced composites has applications in civil engineering and geophysics.

Chadwick and Seet [4] and Singh and Sharma [5] have discussed the propagation of plane harmonic waves in anisotropic thermoelastic materials. Singh [6] studied a problem on wave propagation in an anisotropic generalized thermoelastic solid and obtained a cubic equation, which gives the dimensional velocities of various plane waves. Recently, a number of investigations [7–12] have been carried out using the aforesaid theories of generalized thermoelasticity under the effect of a magnetic field.

Fiber-reinforced composites are used in a variety of structures due to their low weight and high strength. The analysis of stress and deformation of fiber-reinforced composite materials has been an important subject of solid mechanics for the last three decades. Spencer [13], Pipkin [14], and Rogers [15, 16] did pioneering works on the subject. Sengupta and Nath [17] discussed the problem of surface waves in fiber-reinforced anisotropic elastic media. Recently, Singh and Singh [18] discussed the reflection of plane waves at the free surface of a fiber-reinforced elastic half-space.

Fiber-reinforced composites are widely used in engineering structures. A continuum model is used to explain the mechanical properties of such materials. Fibers are assumed as an inherent material property, rather than some form of inclusion in such models [13]. In the case of an elastic solid reinforced by a series of parallel fibers, it is usual to assume transverse isotropy. In the linear case, the associated constitutive relations, and the related infinitesimal stress and strain components, have five material constants as in Abbas [19] and Abbas and Othman [20].

In the present work, the (LS) theory is applied to study the influence of a magnetic field, time, and reinforcement on the total deformation of a body and the interactions with each other. The problem has been solved numerically using a finite element method (FEM). Numerical results for the temperature distribution, displacement, the stress components, and the induced magnetic field are represented graphically.

2 Formulation of the Problem

We consider the problem of a thermoelastic half-space ($x \geq 0$). A magnetic field with a constant intensity $H = (0, 0, H_0)$ acts parallel to the boundary plane (taken as the direction of the z -axis). The surface of the half-space is subjected to a thermal shock which is a function of y and t . Thus, all the quantities considered will be functions of

the time variable t , and of the coordinates x and y . We begin our consideration with linearized equations of electro-dynamics of a slowly moving medium [7]:

$$\mathbf{J} = \text{curl } \mathbf{h} - \varepsilon_0 \dot{\mathbf{E}}, \tag{1}$$

$$\text{curl } \mathbf{E} = -\mu_0 \dot{\mathbf{h}}, \tag{2}$$

$$\mathbf{E} = -\mu_0(\dot{\mathbf{u}} \times \mathbf{H}), \tag{3}$$

$$\nabla \cdot \mathbf{h} = 0. \tag{4}$$

These equations are supplemented by the displacement equations of the theory of elasticity, taking into consideration the Lorentz force, to give

$$\sigma_{ij,j} + F_i = \rho \ddot{u}_i. \tag{5}$$

$$F_i = \mu_0(J \times H)_i, \tag{6}$$

The constitutive equation for a fiber-reinforced linearly thermoelastic anisotropic medium whose preferred direction is that of a unit vector \mathbf{a} is (Belfield et al. [21])

$$\sigma_{ij} = \lambda e_{kk} \delta_{ij} + 2\mu_T e_{ij} + \alpha(a_k a_m e_{km} \delta_{ij} + a_i a_j e_{kk}) + 2(\mu_L - \mu_T)(a_i a_k e_{kj} + a_j a_k e_{ki}) + \beta a_k a_m e_{km} a_i a_j - \beta_{ij}(T - T_0) \delta_{ij}, \quad i, j, k, m = 1, 2, 3, \tag{7}$$

The heat conduction equation is

$$K_{ij} T_{,ij} = \rho c_e (\dot{T} + t_0 \ddot{T}) + T_0 \beta_{ij} (\dot{u}_{i,j} + t_0 \ddot{u}_{i,j}), \quad i, j = 1, 2, 3. \tag{8}$$

where μ_0 is the magnetic permeability; ε_0 is the electric permeability; $\dot{\mathbf{u}}$ is the particle velocity of the medium; \mathbf{h} is the induced magnetic field vector; \mathbf{E} is the induced electric field vector, \mathbf{J} is the current density vector; ρ is the mass density; u_i is the displacement vector components; e_{ij} is the strain tensor; σ_{ij} is the stress tensor; T is the temperature change of a material particle; T_0 is the reference uniform temperature of the body; β_{ij} is the thermal elastic coupling tensor; c_e is the specific heat at constant strain; K_{ij} is the thermal conductivity; t_0 is the relaxation time; δ_{ij} is the Kronecker delta; λ, μ_T are elastic parameters; $\alpha, \beta, (\mu_L - \mu_T)$ are reinforced anisotropic elastic parameters, and $a \equiv (a_1, a_2, a_3)$, and $a_1^2 + a_2^2 + a_3^2 = 1$. The comma notation is used for spatial derivatives, and the superimposed dot represents time differentiation.

We consider the problem of a fiber-reinforced anisotropic half-space ($x \geq 0$). All the considered functions will be depend on the time t and the coordinates x and y . Thus, the displacement vector u_i will have the components,

$$u = u_x = u(x, y, t), \quad v = u_y = v(x, y, t), \quad w = u_z = 0. \tag{9}$$

We choose the fiber direction as $a \equiv (1, 0, 0)$ so that the preferred direction is the x -axis, Eqs. 5–7 simplify, as given below,

$$\sigma_{xx} = (\lambda + 2\alpha + 4\mu_L - 2\mu_T + \beta) \frac{\partial u}{\partial x} + (\lambda + \alpha) \frac{\partial v}{\partial y} - \beta_{11}(T - T_0), \tag{10}$$

$$\sigma_{yy} = (\lambda + 2\mu_T) \frac{\partial v}{\partial y} + (\lambda + \alpha) \frac{\partial u}{\partial x} - \beta_{22}(T - T_0), \tag{11}$$

$$\sigma_{xy} = \mu_L \left(\frac{\partial v}{\partial x} + \frac{\partial u}{\partial y} \right), \tag{12}$$

$$F_x = \mu_0 H_0^2 \left(\frac{\partial^2 u}{\partial x^2} + \frac{\partial^2 v}{\partial x \partial y} - \varepsilon_0 \mu_0 \frac{\partial^2 u}{\partial t^2} \right), \tag{13}$$

$$F_y = \mu_0 H_0^2 \left(\frac{\partial^2 u}{\partial x \partial y} + \frac{\partial^2 v}{\partial y^2} - \varepsilon_0 \mu_0 \frac{\partial^2 v}{\partial t^2} \right), \tag{14}$$

$$\begin{aligned} (A_{11} + \rho R_H^2) \frac{\partial^2 u}{\partial x^2} + (A_{12} + \rho R_H^2) \frac{\partial^2 v}{\partial x \partial y} + A_{13} \frac{\partial^2 u}{\partial y^2} - \beta_{11} \frac{\partial T}{\partial x} \\ = \rho \left(1 + \frac{R_H^2}{c^2} \right) \frac{\partial^2 u}{\partial t^2}, \end{aligned} \tag{15}$$

$$\begin{aligned} (A_{22} + \rho R_H^2) \frac{\partial^2 v}{\partial y^2} + (A_{12} + \rho R_H^2) \frac{\partial^2 u}{\partial x \partial y} + A_{13} \frac{\partial^2 v}{\partial x^2} - \beta_{22} \frac{\partial T}{\partial y} \\ = \rho \left(1 + \frac{R_H^2}{c^2} \right) \frac{\partial^2 v}{\partial t^2}, \end{aligned} \tag{16}$$

$$K_{11} \frac{\partial^2 T}{\partial x^2} + K_{22} \frac{\partial^2 T}{\partial y^2} = \left(\frac{\partial}{\partial t} + t_0 \frac{\partial^2}{\partial t^2} \right) \left(\rho c_e T + T_0 \beta_{11} \frac{\partial u}{\partial x} + T_0 \beta_{22} \frac{\partial v}{\partial y} \right), \tag{17}$$

with

$$\begin{aligned} A_{11} &= \lambda + 2(\alpha + \mu_T) + 4(\mu_L - \mu_T) + \beta, \quad A_{12} = \alpha + \lambda + \mu_L, \quad A_{13} = \mu_L, \\ A_{22} &= \lambda + 2\mu_T, \quad R_H^2 = \frac{\mu_0 H_0^2}{\rho}, \quad c^2 = \frac{1}{\varepsilon_0 \mu_0}, \quad \beta_{11} = (2\lambda + 3\alpha + 4\mu_L - 2\mu_T + \beta) \\ \alpha_{11} + (\lambda + \alpha)\alpha_{22}, \quad \beta_{22} &= (2\lambda + \alpha)\alpha_{11} + (\lambda + 2\mu_T)\alpha_{22}. \end{aligned}$$

where the coefficients of linear thermal expansion are α_{11}, α_{22} . For convenience, the following non-dimensional variables are used:

$$\begin{aligned} (x', y', u', v') &= c_1 \chi(x, y, u, v), \quad t' = c_1^2 \chi t, \quad T' = \frac{\beta_{11}(T - T_0)}{\rho c_1^2}, \quad \chi = \frac{\rho c_e}{K_{11}}, \quad h' = \frac{h}{H_0}, \\ c_1^2 &= \frac{A_{11}}{\rho}, \quad (\sigma'_{xx}, \sigma'_{xy}, \sigma'_{yy}) = \frac{1}{\rho c_1^2} (\sigma_{xx}, \sigma_{xy}, \sigma_{yy}). \end{aligned} \tag{18}$$

In terms of the non-dimensional quantities defined in Eq. 18, the above governing equations reduce to (dropping the dashed for convenience)

$$\sigma_{xx} = \frac{\partial u}{\partial x} + B_1 \frac{\partial v}{\partial y} - T, \tag{19}$$

$$\sigma_{yy} = B_1 \frac{\partial u}{\partial x} + B_2 \frac{\partial v}{\partial y} - B_3 T, \tag{20}$$

$$\sigma_{xy} = B_4 \left(\frac{\partial v}{\partial x} + \frac{\partial u}{\partial y} \right), \tag{21}$$

$$\frac{\partial \sigma_{xx}}{\partial x} + \frac{\partial \sigma_{xy}}{\partial y} + \eta \left(\frac{\partial^2 u}{\partial x^2} + \frac{\partial^2 v}{\partial x \partial y} \right) = \xi \frac{\partial^2 u}{\partial t^2}, \tag{22}$$

$$\frac{\partial \sigma_{xy}}{\partial x} + \frac{\partial \sigma_{yy}}{\partial y} + \eta \left(\frac{\partial^2 u}{\partial x \partial y} + \frac{\partial^2 v}{\partial y^2} \right) = \xi \frac{\partial^2 v}{\partial t^2}, \tag{23}$$

$$\frac{\partial^2 T}{\partial x^2} + \varepsilon_1 \frac{\partial^2 T}{\partial y^2} = \left(\frac{\partial}{\partial t} + t_0 \frac{\partial^2}{\partial t^2} \right) \left(T + \varepsilon_2 \frac{\partial u}{\partial x} + \varepsilon_3 \frac{\partial v}{\partial y} \right). \tag{24}$$

where $(B_1, B_2, B_4) = \frac{1}{A_{11}}(A_{12}, A_{22}, A_{13})$, $B_3 = \frac{\beta_{22}}{\beta_{11}}$, $\xi = 1 + \frac{R_H^2}{c^2}$, $\eta = \frac{R_H^2}{c_1^2}$, $(\varepsilon_2, \varepsilon_3) = \frac{T_0 \beta_{11}}{A_{11} \rho c_e}(\beta_{11}, \beta_{22})$, $\varepsilon_1 = \frac{K_{11}}{K_{22}}$,

3 Finite Element Formulation

In this section, the governing equations of generalized magneto-thermoelasticity (the LS theory) are summarized, followed by the corresponding finite element equations. In the finite element method, the displacement components, u , v , and temperature, T , are related to the corresponding nodal values by

$$u = \sum_{i=1}^m N_i u_i(t), \quad v = \sum_{i=1}^m N_i v_i(t), \quad T = \sum_{i=1}^m N_i T_i(t). \tag{25}$$

where m denotes the number of nodes per element and N_i 's are the shape functions. The eight-node isoparametric, quadrilateral element is used for displacement components and temperature calculations. The weighting functions and the shape functions coincide. Thus,

$$\delta u = \sum_{i=1}^m N_i \delta u_i, \quad \delta v = \sum_{i=1}^m N_i \delta v_i, \quad \delta T = \sum_{i=1}^m N_i \delta T_i, \tag{26}$$

It should be noted that appropriate boundary conditions associated with the governing Eqs. 22–24 must be adopted in order to properly formulate a problem. Boundary conditions are either essential (or geometric) or natural (or traction) types. Essential conditions are prescribed displacements u , v , and temperature T , while the natural boundary conditions are prescribed tractions and heat flux which are expressed as

$$\sigma_{xx} n_x + \sigma_{xy} n_y = \bar{\tau}_x, \quad \sigma_{xy} n_x + \sigma_{yy} n_y = \bar{\tau}_y, \quad q_x n_x + q_y n_y = \bar{q}. \tag{27}$$

where n_x and n_y are direction cosines of the outward unit normal vector at the boundary, $\bar{\tau}_x$, $\bar{\tau}_y$ are the given traction values, and \bar{q} is the given surface flux.

In the absence of a body force, considering the Lorentz force F_i , the governing equations are multiplied by weighting functions and then are integrated over the spatial

domain Ω with the boundary Γ . Applying integration by parts and making use of the divergence theorem reduce the order of the spatial derivatives and allow for the application of the boundary conditions. Thus, the finite element equations corresponding to Eqs. 22–24 can be obtained as

$$\int_{\Omega} \left\{ \begin{array}{l} \frac{\partial \delta u}{\partial x} \sigma_{xx} + \frac{\partial \delta u}{\partial y} \sigma_{xy} \\ \frac{\partial \delta v}{\partial x} \sigma_{xy} + \frac{\partial \delta v}{\partial y} \sigma_{yy} \\ \left(\frac{\partial \delta T}{\partial x} \frac{\partial T}{\partial x} + \varepsilon_1 \frac{\partial \delta T}{\partial y} \frac{\partial T}{\partial y} \right) \end{array} \right\} d\Omega + \int_{\Omega} \left\{ \begin{array}{l} \delta u \left(\xi \frac{\partial^2 u}{\partial t^2} - \eta \left(\frac{\partial^2 u}{\partial x^2} + \frac{\partial^2 v}{\partial x \partial y} \right) \right) \\ \delta v \left(\xi \frac{\partial^2 v}{\partial t^2} - \eta \left(\frac{\partial^2 u}{\partial x \partial y} + \frac{\partial^2 v}{\partial y^2} \right) \right) \\ \delta T \left(\frac{\partial}{\partial t} + t_0 \frac{\partial^2}{\partial t^2} \right) \left(T + \varepsilon_2 \frac{\partial u}{\partial x} + \varepsilon_3 \frac{\partial v}{\partial y} \right) \end{array} \right\} d\Omega$$

$$= \int_{\Gamma} \left\{ \begin{array}{l} \delta u \bar{\tau}_x \\ \delta v \bar{\tau}_y \\ \delta T \bar{q} \end{array} \right\} d\Gamma, \tag{28}$$

Substituting the constitutive relations, Eqs 19–21, and Eqs. 25–26 into Eq. 28 leads to

$$\sum_{e=1}^{me} \left(\begin{bmatrix} M_{11}^e & 0 & 0 \\ 0 & M_{22}^e & 0 \\ M_{31}^e & M_{32}^e & M_{33}^e \end{bmatrix} \begin{Bmatrix} \dot{u}^e \\ \dot{v}^e \\ \dot{T}^e \end{Bmatrix} + \begin{bmatrix} 0 & 0 & 0 \\ 0 & 0 & 0 \\ C_{31}^e & C_{32}^e & C_{33}^e \end{bmatrix} \begin{Bmatrix} u^e \\ v^e \\ T^e \end{Bmatrix} + \begin{bmatrix} K_{11}^e & K_{12}^e & K_{13}^e \\ K_{21}^e & K_{22}^e & K_{23}^e \\ 0 & 0 & K_{33}^e \end{bmatrix} \begin{Bmatrix} u^e \\ v^e \\ T^e \end{Bmatrix} = \begin{Bmatrix} F_1^e \\ F_2^e \\ F_3^e \end{Bmatrix} \right). \tag{29}$$

where me is the total number of elements. The coefficients in Eq. 29 are given below.

$$M_{11}^e = \int_{\Omega} \xi [N]^T [N] d\Omega, \quad M_{22}^e = \int_{\Omega} \xi [N]^T [N] d\Omega,$$

$$M_{31}^e = \int_{\Omega} t_0 \varepsilon_2 [N]^T \left[\frac{\partial N}{\partial x} \right] d\Omega,$$

$$M_{32}^e = \int_{\Omega} t_0 \varepsilon_3 [N]^T \left[\frac{\partial N}{\partial y} \right] d\Omega, \quad M_{33}^e = \int_{\Omega} t_0 [N]^T [N] d\Omega,$$

$$C_{31}^e = \int_{\Omega} \varepsilon_2 [N]^T \left[\frac{\partial N}{\partial x} \right] d\Omega,$$

$$C_{32}^e = \int_{\Omega} \varepsilon_3 [N]^T \left[\frac{\partial N}{\partial y} \right] d\Omega, \quad C_{33}^e = \int_{\Omega} [N]^T [N] d\Omega,$$

$$K_{11}^e = \int_{\Omega} \left(\left[\frac{\partial N}{\partial x} \right]^T \left[\frac{\partial N}{\partial x} \right] + B_4 \left[\frac{\partial N}{\partial y} \right]^T \left[\frac{\partial N}{\partial y} \right] - \eta [N]^T \left[\frac{\partial^2 N}{\partial x^2} \right] \right) d\Omega,$$

$$K_{12}^e = \int_{\Omega} \left(B_1 \left[\frac{\partial N}{\partial x} \right]^T \left[\frac{\partial N}{\partial y} \right] + B_4 \left[\frac{\partial N}{\partial y} \right]^T \left[\frac{\partial N}{\partial x} \right] - \eta [N]^T \left[\frac{\partial^2 N}{\partial x \partial y} \right] \right) d\Omega,$$

$$\begin{aligned}
 K_{13}^e &= \int_{\Omega} - \left[\frac{\partial N}{\partial x} \right]^T [N] d\Omega, & K_{23}^e &= \int_{\Omega} -B_3 \left[\frac{\partial N}{\partial y} \right]^T [N] d\Omega, \\
 K_{21}^e &= \int_{\Omega} \left(B_4 \left[\frac{\partial N}{\partial x} \right]^T \left[\frac{\partial N}{\partial y} \right] + B_1 \left[\frac{\partial N}{\partial y} \right]^T \left[\frac{\partial N}{\partial x} \right] - \eta [N]^T \left[\frac{\partial^2 N}{\partial x \partial y} \right] \right) d\Omega, \\
 K_{22}^e &= \int_{\Omega} \left(B_4 \left[\frac{\partial N}{\partial x} \right]^T \left[\frac{\partial N}{\partial x} \right] + B_2 \left[\frac{\partial N}{\partial y} \right]^T \left[\frac{\partial N}{\partial y} \right] - \eta [N]^T \left[\frac{\partial^2 N}{\partial y^2} \right] \right) d\Omega, \\
 K_{33}^e &= \int_{\Omega} \left(\left[\frac{\partial N}{\partial x} \right]^T \left[\frac{\partial N}{\partial x} \right] + \varepsilon_1 \left[\frac{\partial N}{\partial y} \right]^T \left[\frac{\partial N}{\partial y} \right] \right) d\Omega, \\
 F_1^e &= \int_{\Gamma} [N]^T \bar{t}_x d\Gamma, & F_2^e &= \int_{\Gamma} [N]^T \bar{t}_y d\Gamma, & F_3^e &= \int_{\Gamma} [N]^T \bar{q} d\Gamma.
 \end{aligned}$$

Symbolically, the discretized equations of Eq. 29 can be written as

$$M \ddot{d} + C \dot{d} + K d = F^{\text{ext}}. \tag{30}$$

where M , C , K , and F^{ext} represent the mass, damping, stiffness matrices, and external force vectors, respectively; $d = [uvT]^t$. On the other hand, the time derivatives of the unknown variables have to be determined by the Newmark time integration method (see Wriggers [22]).

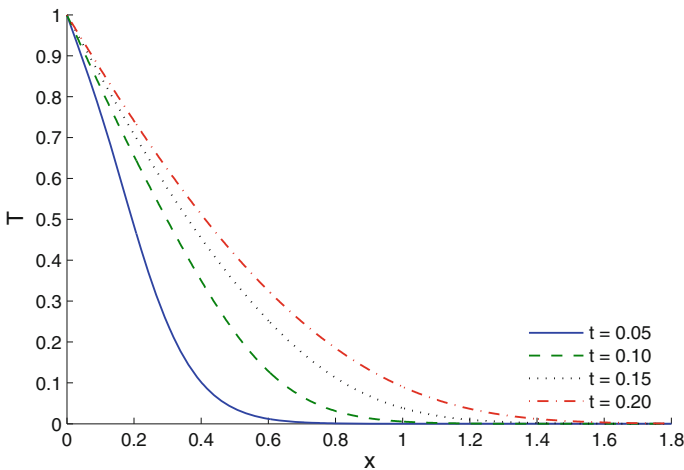


Fig. 1 Temperature distribution for different values of t at $y = 1$

4 Application

We consider the problem of a half-space Ψ , which is defined as follows:

$$\Psi = \{(x, y, z) : 0 \leq x < \infty, -\infty < y < \infty, -\infty < z < \infty\}.$$

The surface of the half-space is taken to be traction free, and the thermal shock $g(y, t)$ applied on the surface at $x = 0$ is taken of the form,

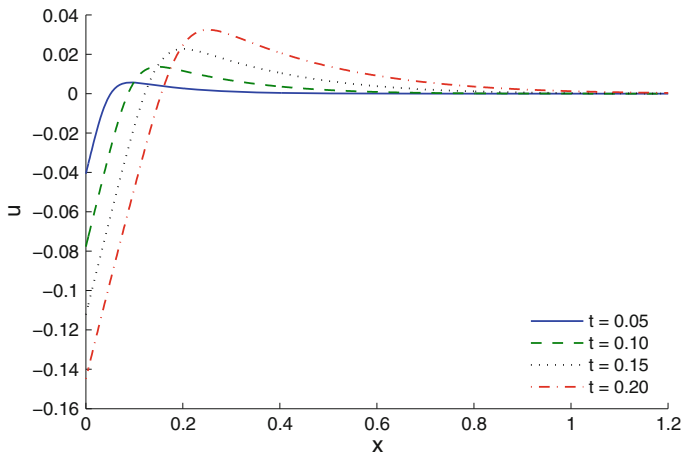


Fig. 2 Horizontal displacement distribution, u , for different values of t at $y = 1$

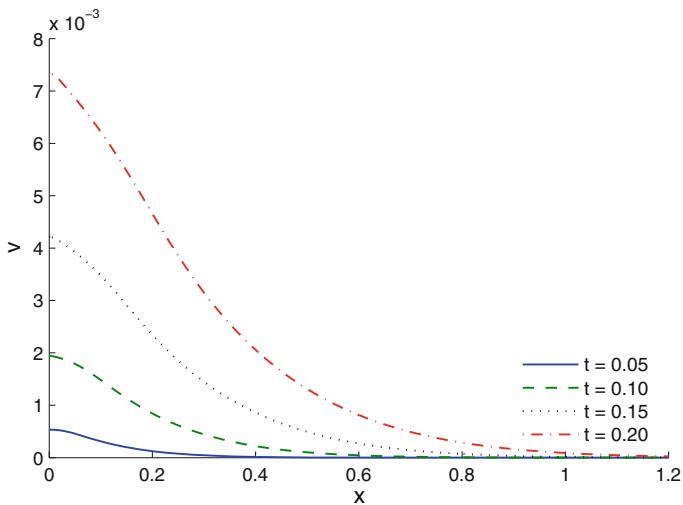


Fig. 3 Vertical displacement distribution v for different values of t at $y = 1$

$$g(y, t) = T_1 H(t) H(l - |y|), \tag{31}$$

where H is the Heaviside unit step function and T_1 is a constant. This means that heat is applied on the surface of the half-space on a narrow band of width $2l$ surrounding the y -axis to keep it at temperature T_1 , while the rest of the surface is kept at zero temperature. We assume the following initial conditions:

$$u = v = T = 0, \quad t = 0, \quad \dot{u} = \dot{v} = \dot{T} = 0, \quad t = 0. \tag{32}$$

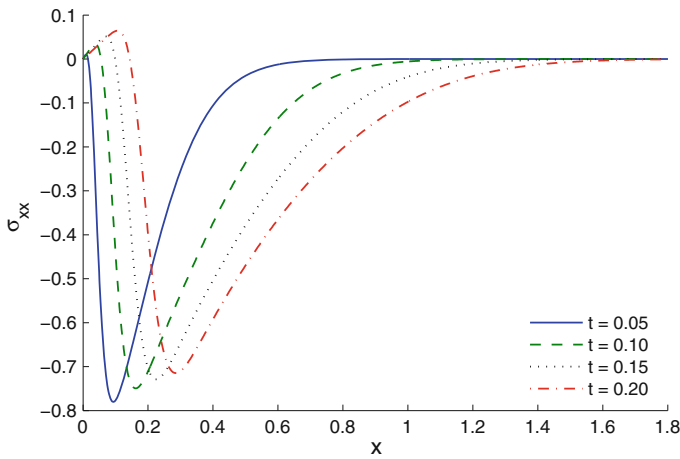


Fig. 4 Distribution of stress component σ_{xx} for different values of t at $y = 1$

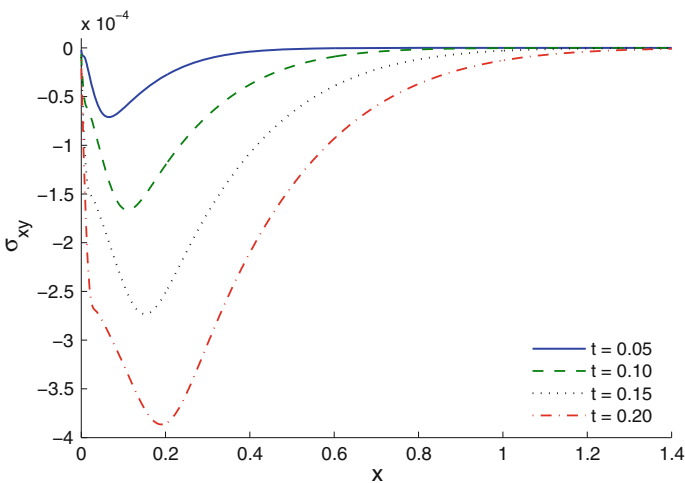


Fig. 5 Distribution of stress component σ_{xy} for different values of t at $y = 1$

5 Numerical Example

To study the effect of reinforcement on wave propagation, we use the following physical constants for generalized fiber-reinforced thermoelastic materials.

$$\begin{aligned} \lambda &= 5.65 \times 10^{10} \text{ N} \cdot \text{m}^{-2}, \mu_T = 2.46 \times 10^{10} \text{ N} \cdot \text{m}^{-2}, \mu_L = 5.66 \times 10^{10} \text{ N} \cdot \text{m}^{-2}, \\ \alpha &= -1.28 \times 10^{10} \text{ N} \cdot \text{m}^{-2}, \beta = 220.90 \times 10^{10} \text{ N} \cdot \text{m}^{-2}, \alpha_{11} = 0.017 \times 10^{-4} \text{ K}^{-1}, \\ \alpha_{22} &= 0.015 \times 10^{-4} \text{ K}^{-1}, c_e = 0.787 \times 10^3 \text{ J} \cdot \text{kg}^{-1} \cdot \text{K}^{-1}, T_0 = 293 \text{ K}, T_1 = 1, \\ K_{11} &= 0.0921 \times 10^3 \text{ J} \cdot \text{m}^{-1} \cdot \text{s}^{-1} \cdot \text{K}^{-1}, K_{22} = 0.0963 \times 10^3 \text{ J} \cdot \text{m}^{-1} \cdot \text{s}^{-1} \cdot \text{K}^{-1}, \\ R_H^2 &= 0.02c_1^2, l = 1, \rho = 2660 \text{ kg} \cdot \text{m}^{-3}. \end{aligned}$$

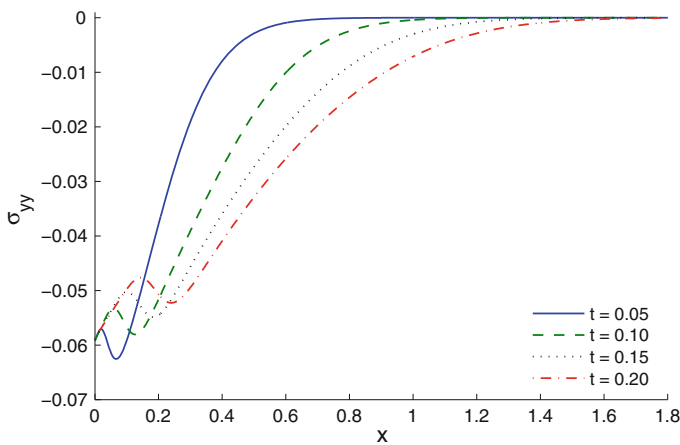


Fig. 6 Distribution of stress component σ_{yy} for different values of t at $y = 1$

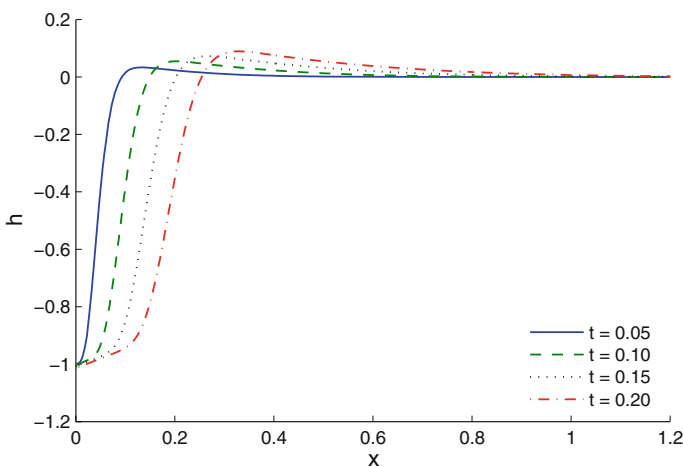


Fig. 7 Distribution of induced magnetic field, h , for different values of t at $y = 1$

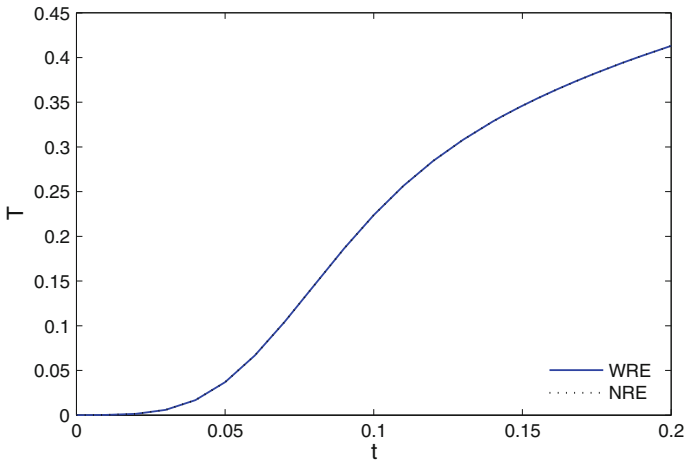


Fig. 8 Temperature distribution at $x = 0.5$ and $y = 1$

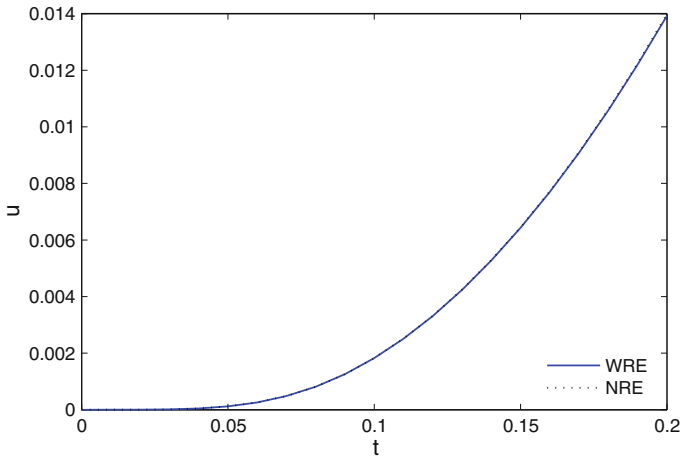


Fig. 9 Horizontal displacement distribution, u , at $x = 0.5$ and $y = 1$

The field quantities, temperature, displacement components, u, v , stress components, $\sigma_{xx}, \sigma_{yy}, \sigma_{xy}$, and induced magnetic field, h , depend not only on space x and time t but also on the thermal relaxation time t_0 . Here all the variables are taken in non-dimensional forms. The grid size has been refined until the values of u, v , and T stabilize. Further refinement of mesh size over 100×100 elements does not change the values considerably, which is therefore accepted as the grid size for computing purposes. Figures 1, 2, 3, 4, 5, 6, and 7 exhibit the variation of the temperature, displacement components, u, v , and stress components, $\sigma_{xx}, \sigma_{yy}, \sigma_{xy}$, and induced magnetic field, h , with space x under Lord–Shulman’s theory (LS), i.e., when there is one thermal relaxation time ($t_0 = 0.02$) at $y = 1$ for four different values of time ($t = 0.05, 0.1, 0.15, 0.2$). Figures 1 and 3 show that the time has an increasing effect

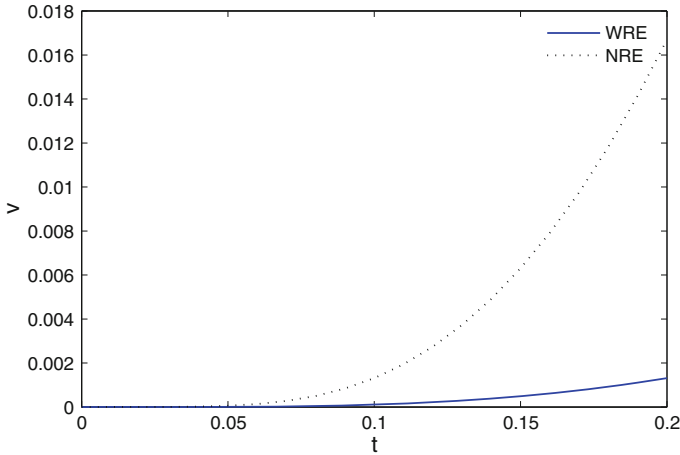


Fig. 10 Vertical displacement distribution, v , at $x = 0.5$ and $y = 1$

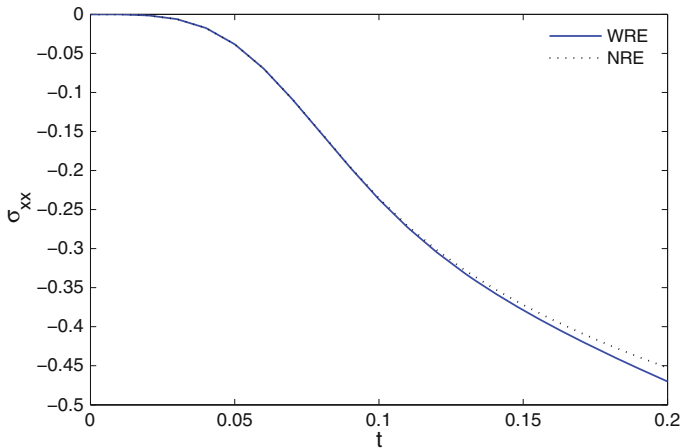


Fig. 11 Distribution of stress component σ_{xx} at $x = 0.5$ and $y = 1$

on the temperature and displacement component v with the (LS) theory. Figures 2 and 7 depict that the time has a decreasing effect on the displacement component, u , and the induced magnetic field, h , for $0 < x < 0.2$ and an increasing effect for $0.2 < x < 1.2$. Figures 4 and 6 show that the time has an increasing effect on the two components of stress σ_{xx} and σ_{yy} for $0 < x < 0.2$ and a decreasing effect for $0.2 < x < 1.2$. Figure 5 shows that the time has a decreasing effect on the stress component σ_{xy} . We have found that the time has a significant effect on the field quantities. Figures 7, 8, 9, 10, 11, and 12 show the variation of the temperature, displacement components, u , v , and stress components, σ_{xx} , σ_{yy} , σ_{xy} , and induced magnetic field, h , with time t at

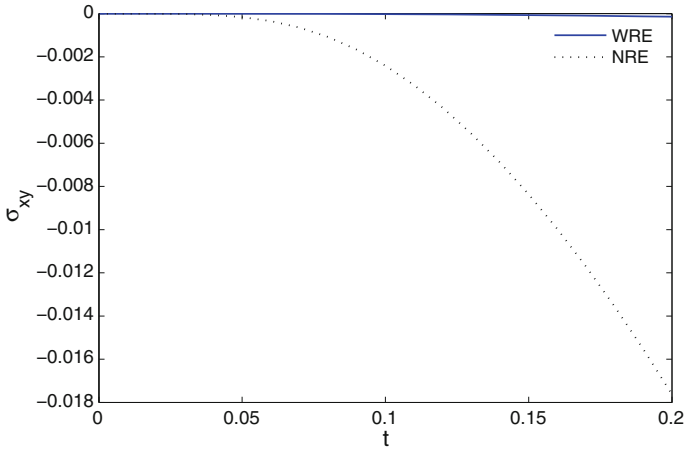


Fig. 12 Distribution of stress component σ_{xy} at $x = 0.5$ and $y = 1$

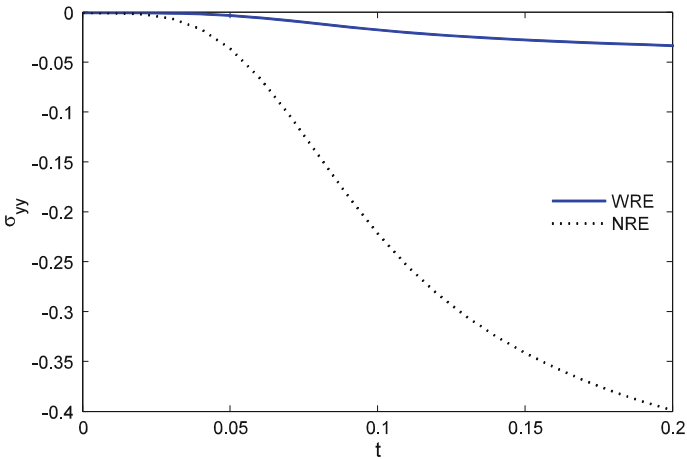


Fig. 13 Distribution of stress component σ_{yy} at $x = 0.5$ and $y = 1$

$x = 0.5$ and $y = 1$ under Lord–Shulman’s theory (LS) with reinforcement (WRE) and without reinforcement (NRE). In Figs. 8, 9, 10, 11, 12, 13, and 14, the solid lines refer to the case with reinforcement (WRE) and the dotted lines refer to the case without reinforcement (NRE), i.e., $(\alpha = 0, \beta = 0, \text{ and } (\mu_L - \mu_T) = 0)$. It is easy to see from Figs. 8 and 9 that the reinforcement has a small effect on the physical quantities, temperature and displacement components u for $0 < t < 0.2$. Figures 10 and 11 show that the reinforcement has a decreasing effect on the displacement components v and the stress component σ_{xx} for $0 < t < 0.2$. Figures 12, 13, and 14 show that the reinforcement has an increasing effect on the stress components, σ_{xy} , σ_{yy} , and induced magnetic field, h .

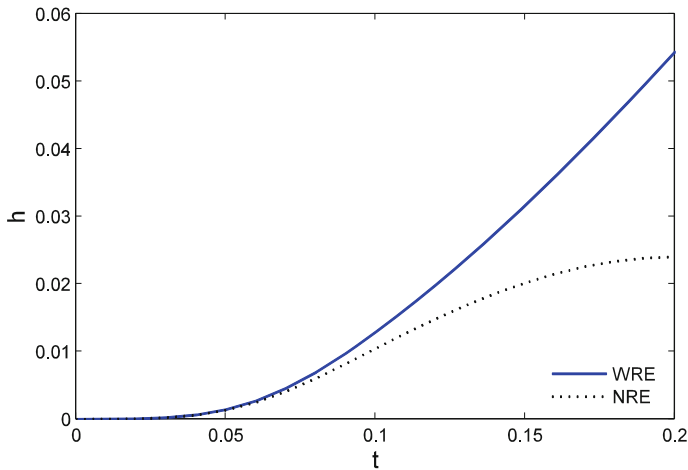


Fig. 14 Distribution of induced magnetic field, h , at $x = 0.5$ and $y = 1$

6 Concluding Remarks

In this work, the finite element method is used to study the problem of the effect of a magnetic field on a thermal shock problem at the free surface of a fiber-reinforced thermoelastic half-space under the Lord–shulman theory. We can obtain the following conclusions based on the above analysis:

1. The time has a significant effect on the field quantities.
2. The reinforcement has a great effect on the distribution of field.

References

1. H.W. Lord, Y. Shulman, *J. Mech. Phys. Solids* **15**, 299 (1967)
2. R.S. Dhaliwal, H.H. Sherief, *Q. Appl. Math.* **33**, 1 (1980)
3. A.U. Erdem, Heat Conduction in Fiber-Reinforced Rigid Bodies, 10 Ulusal Ist Bilimi ve Tekmgi Kongrest (ULIBTK), 6–8 Eylul, Ankara (1995)
4. P. Chadwick, L.T.C. Seet, *Mathematica* **17**, 255 (1970)
5. H. Singh, J.N. Sharma, *J. Acoust. Soc. Am.* **77**, 1046 (1985)
6. B. Singh, *J. Pure Appl. Math.* **34**, 1479 (2003)
7. M. Ezzat, M.I.A. Othman, A. El Karamany, *J. Therm. Stress.* **24**, 411 (2001)
8. M.I.A. Othman, *Acta Mech.* **169**, 37 (2004)
9. I.A. Abbas, A.N. Abd-alla, *Arch. Appl. Mech.* **78**, 283 (2008)
10. I.A. Abbas, *Forsch Ingenieurwes* **71**, 215 (2007)
11. M.I.A. Othman, K.h. Lotfy, R.M. Farouk, *Int. J. Ind. Math.* **1**, 87 (2009)
12. M.I.A. Othman, K.h. Lotfy, R.M. Farouk, *Acta Phys. Pol. A* **116**, 185 (2009)
13. A.J.M. Spencer, *Deformation of Fibre-Reinforced Materials* (Clarendon, Oxford, 1941)
14. A.C. Pipkin, Finite deformations of ideal fiber-reinforced composites, in *Composites Materials*, 2, ed. by G.P. Sendeckyj (Academic, New York, 1973), pp. 251–308
15. T.G. Rogers, Finite deformations of strongly anisotropic materials, in *Theoretical Rheology*, ed. by J.R.A. Pearson, K. Walters, J.F. Hutton (Applied Science Publishers, London, 1975), pp. 141–168
16. T.G. Rogers, Anisotropic elastic and plastic materials, in *Continuum Mechanics Aspects of Geodynamics and Rock Fracture Mechanics*, ed. by P. Thoft-Christensen (Reidel, Dordrecht, 1975), pp. 177–200

17. P.R. Sengupta, S. Nath, Sadhana, Proc. Indian Acad. Sci. **26**, 363 (2001)
18. B. Singh, S.J. Singh, Sadhana, Proc. Indian Acad. Sci. **29**, 249 (2004)
19. I.A. Abbas, Arch. Appl. Mech. **79**, 41 (2008)
20. I.A. Abbas, M.I.A. Othman, Int. J. Ind. Math. **1**, 121 (2009)
21. A.J. Belfield, T.G. Rogers, A.J.M. Spencer, J. Mech. Phys. Solids **31**, 25 (1983)
22. P. Wriggers, *Nonlinear Finite Element Methods* (Springer, Berlin, 2008)